Voltammetric and Coulometric Studies of the Mechanism of Electrohydrodimerization of Diethyl Fumarate in Dimethylformamide Solutions

W. V. Childs,*[,1] J. T. Maloy,[2] C. P. Keszthelyi, and Allen J. Bard*

Department of Chemistry, The University of Texas at Austin, Austin, Texas 78712

Reprinted from JOURNAL OF THE ELECTROCHEMICAL SOCIETY
Vol. 118, No. 6, June 1971
Printed in U.S.A.

Voltammetric and Coulometric Studies of the Mechanism of Electrohydrodimerization of Diethyl Fumarate in Dimethylformamide Solutions

W. V. Childs,*[1] J. T. Maloy,[2] C. P. Keszthelyi, and Allen J. Bard*

Department of Chemistry, The University of Texas at Austin, Austin, Texas 78712

ABSTRACT

The reduction of diethyl fumarate (DEF) in tetra-n-butylammonium iodide (TBAI)-dimethylformamide (DMF) solutions at a platinum electrode has been studied by cyclic voltammetry, double potential step chronoamperometry, and controlled potential coulometry. The chronoamperometric response for several possible mechanisms of electrohydrodimerization has been obtained by digital simulation techniques, and a method for distinguishing among the mechanisms suggested. Results of double potential step chronoamperometric experiments strongly support a mechanism where the electrochemically generated anion radicals undergo a second-order dimerization reaction. Controlled potential electrolysis results give evidence for a bulk polymerization reaction in the absence of proton donor; protonation in the presence of hydroquinones; and good efficiency to the hydrodimer product in the presence of lithium perchlorate trihydrate.

The study of electrohydrodimerizations (or electrolytic reductive couplings) of activated olefins and related substances, by an over-all reaction shown in Eq. [1] has been the subject of numerous investigations, most recently especially

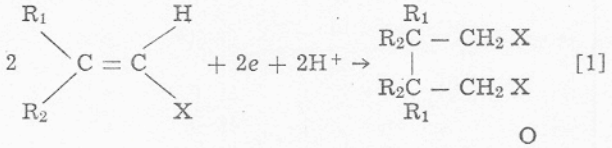

[1]

X = electron-withdrawing group, *e.g.* —CN, —C(=O)—OEt

by Baizer and co-workers [see (1-3) and references contained therein]. The reduction on acrylonitrile ($R_1 = R_2 = H$, X = CN) has been the subject of most of the investigations because of the commercial importance of the hydrodimerized product, adiponitrile. Relatively few studies have been concerned with a kinetic analysis of the mechanism of the process, however. The first papers, generally on the basis of product distribution, viewed the process as occurring with an initial two-electron reduction to the dianion, which then attacked the parent molecule to produce coupled products. Beck (4), based on an analysis of current-potential curves for the reduction of acrylonitrile, proposed a rate-determining step involving one electron and one water molecule to form a neutral radical, which is immediately reduced further to the protonated carbanion. Recently Petrovich, Baizer, and Ort (2, 3) carried out polarographic, cyclic voltammetric, and macroscale electrolysis studies of a number of diactivated olefins in N,N-dimethylformamide (DMF) solutions and concluded that dimeric products were formed by either attack of an electrochemically generated anion radical on the parent unreduced olefin, followed by further electroreduction and protonation, or by protonation of the anion radical, followed by further reduction to an anion and subsequent attack on the olefin. An alternate pathway to the dimer, that of coupling of the anion radicals, was deemed less likely.

The research described here was undertaken to investigate the mechanism of the hydrodimerization reaction using a variety of electroanalytical techniques,

* Electrochemical Society Active Member.

[1] Present address: Phillips Petroleum Company, Bartlesville, Oklahoma, 74004.

[2] Present address: Department of Chemistry, West Virginia University, Morgantown, West Virginia.

Key words: electrolytic hydrodimerization, potential step chronoamperometry, cyclic voltammetry, coulometry, computer simulation.

including double potential step chronoamperometry, cyclic voltammetry, and controlled potential coulometry. Other investigations of the mechanism by rotating ring disk electrode voltammetry and electron spin resonance spectroscopy will be reported elsewhere. The compound selected for study was diethyl fumarate (DEF), since

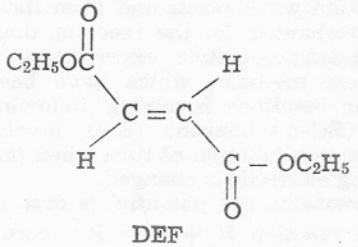

DEF

previous studies (2, 3) have shown that the following reactions of the initially formed radical anion are sufficiently slow to allow rather easy application of electroanalytical techniques.

Experimental

Materials.—Dimethylformamide (DMF) was purified as previously described (5). Tetra-n-butylammonium iodide (TBAI) was the polarographic grade supplied by Southwestern Analytical Chemicals, Austin, Texas. Diethyl fumarate (DEF) (K and K Laboratories, Inc., Plainview, New York) was used without further purification, since preliminary experiments with distilled samples showed identical behavior to that of unpurified samples.

Apparatus.—The cell used in coulometric experiments is shown in Fig. 1. It is comprised of four compartments (auxiliary, intermediate-buffer, working, and reference,) four electrodes (auxiliary, micro, macro, and reference), and a freeze-pump-thaw (F-P-T) chamber. The F-P-T chamber is used for degassing the solution by freezing at liquid nitrogen temperature, pumping to about 10^{-5} Torr, and then thawing to room temperature (with the pump off). This procedure is repeated three to five times (5).

A silver wire isolated in a compartment closed with a fine sintered glass disk was used as a reference electrode. It was found to be stable (with less than a 10 mV drift) in our TBAI-DMF systems for at least 48 hr. The reference electrode was positioned in the current path between the auxiliary and macroelectrode so that the macroelectrode would not overshoot the controlled voltage because of iR drops in coulometry experiments.

The microelectrode used for chronoamperometry and voltammetry was an 0.16 cm diameter platinum disk in glass. It was pretreated by soaking briefly in nitric acid, rinsing, and drying. The macroelectrode was two thicknesses of fine platinum gauze, 2 cm high by 10 cm long, formed into a "C." It was attached with a pin

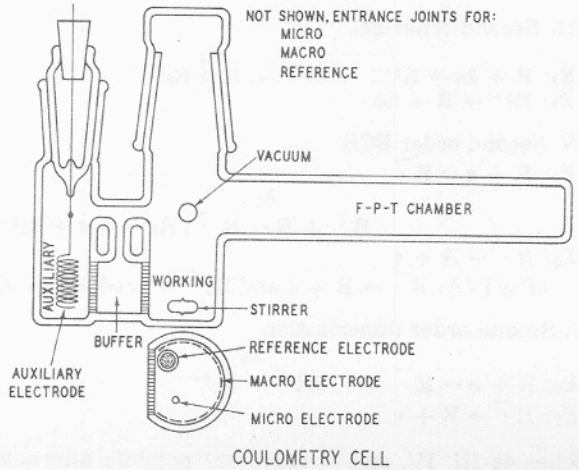

Fig. 1. Coulometry cell

socket for easy cleaning and assembly. The auxiliary electrode was 20 cm of coiled 18 gauge platinum wire. Stirring was accomplished with a Teflon-coated stirring bar (5/16 in. diameter by 1/2 in. long). Some chronoamperometric meaurements were performed in a cell similar to the one shown in Fig. 1, but with only two large compartments (F-P-T and working), with the auxiliary electrode housed in a fritted chamber similar to that used with the reference electrode described above, but having a medium, rather than fine, sintered glass disk on the bottom.

Electrochemical experiments were carried out with a PAR Model 170 Electrochemistry System (Princeton Applied Research Corporation, Princeton, New Jersey). Positive feedback was generally used for resistance compensation in voltammetric experiments. In some high current situations during macroelectrolysis at high concentrations compensation was not complete because of limitations in the instrument. This does not affect the results, however, since it resulted in actual potentials less negative than those set. The various functions of the instrument were checked and calibrated periodically.

Some chronoamperometric data were also taken using a Wenking Model 61-RH potentiostat in conjunction with a Wavetek Model 114 function generator and associated switching and triggering circuitry.

Most of the chronoamperometric and chronocoulometric data were recorded using a PDP-12A computer (Digital Equipment Corporation, Maynard, Massachusetts) for data acquisition. Signals for current and coulombs from the PAR-170 system were interfaced to the analog-to-digital converters of the PDP-12A through appropriate operational amplifier followers, sense line triggers, etc. Data points were taken every 50 μsec. Techniques employed were generally similar to previous applications of digital data acquisition techniques in chronocoulometric experiments [see (6, 7) and references contained therein].

Typical experimental procedure.—A solution of DEF in DMF was prepared in a 50 ml volumetric flask. When lithium perchlorate was to be added to the electrolysis solution, a weighed amount of $LiClO_4 \cdot 3H_2O$ was added to the F-P-T chamber and 4.00g of TBAI was placed in the bottom of the working electrode compartment along with the stirring bar. The TBAI could not be mixed with the $LiClO_4$ at this stage, as lithium iodide will air oxidize to give iodine.

The cell was set up with the F-P-T chamber vertical and the DEF-DMF solution was poured in. The cell was then assembled by inserting the electrodes, closed and evacuated, and the F-P-T cycles were carried out. It was then manipulated to mix the TBAI and liquid (50 ml of DMF solution and 4.00g TBAI result in a volume of 53.0 ml).

The cell was then righted, the levels in the different compartments adjusted roughly by sloshing, and then the cell was set on a flat, stable surface and allowed to equilibrate thermally and hydrostatically; this took about 2 hr. In this cell 42% of the solution was in the working electrode compartment, as determined by removing the contents of each chamber and weighing them. The reference compartment was filled by means of a small hole just above, and a larger hole about 2 cm above, the electrolyte level. All electrochemical experiments were performed with the solution under reduced pressure. During coulometry the cell was maintained at 20°-25° and was stirred continuously. To prevent condensation in the remote portions of the cell, the liquid had to be kept cooler than the dry portions of the cell as transport through the vapor space was rapid at the reduced pressure.

Results

Cyclic voltammetry.—Cyclic voltammetric experiments were undertaken to determine the potentials for the potential-step experiments, to provide qualitative and semiquantitative information for use in

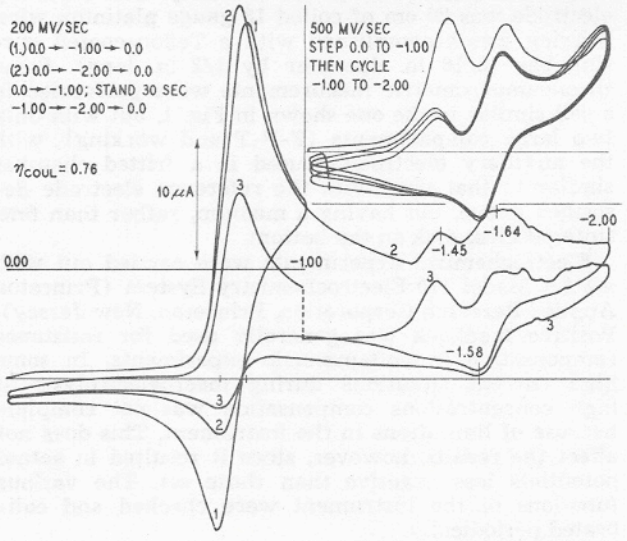

Fig. 2. Cyclic voltammograms for DEF in 0.44M TBAI-DMF solution. Potential programs and sweep rates as shown.

determining the effects of different additives (water, $LiClO_4$), and for following macroscale electrolyses. Typical cyclic voltammograms of DEF in anhydrous DMF containing 0.44*M* TBAI are shown in Fig. 2. The first peak occurs at a cathodic peak potential, E_{pc}, of −0.80V *vs.* the Ag reference electrode (Ag-RE). In all of the solutions studied the range of the peak potential was −0.78 to −0.81V with sweep rates of 100-200 mV/sec (and with positive feedback used for resistance compensation). Half-peak potentials were typically 60 mV positive of E_{pc}; $E_{pc} - E_{pa}$ values were typically 65-67 mV. Baizer and co-workers (3) gave −1.54V *vs.* an aqueous saturated calomel electrode (SCE) for the polarographic $E_{1/2}$ of the first wave in DMF −0.1*M* tetraethylammonium perchlorate (TEAP) solutions—both anhydrous and containing 1*M* water. Smaller waves following the first occur at about −1.45 and −1.64V *vs.* Ag-RE. Baizer and co-workers (3) found that a current decrease was noted during polarographic reduction of DEF at potentials about 0.6V past the $E_{1/2}$ of the first wave in anhydrous DMF. They ascribed this behavior to formation of the dianion at these potentials which reacted with incoming parent molecules in a polymerization reaction. In DMF solutions containing 1*M* H_2O a second wave, somewhat smaller than the first wave, at −2.27V *vs.* SCE, was observed. Typical data for the variation of the cathodic peak current, i_{pc}, of the first reduction with scan rate, v, and concentration, C, are given in Table I. Baizer and co-workers (3) mention a similar decrease of $i_{pc}/v^{1/2}$ *C* with increasing v for DEF and related compounds.

Table I. Typical cyclic voltammetric data for first reduction wave of diethyl fumarate[a]

Concentration, C (mM)	Scan rate, v (V/sec)	Peak current, i_{pc} (μA)	$i_{pc}/v^{1/2}C$
1.71	0.10	43	8.0
	0.20	60	7.8
	0.50	91	7.6
	1.00	128	7.5
	2.00	171	7.1
	5.00	262	6.8
2.03	0.02	23	8.0
	0.05	36	8.0
	0.10	51	7.9
	0.20	71	7.8
	0.50	105	7.3
3.31	0.05	62	8.4
	0.10	85	8.0
	0.20	118	8.0
	0.50	178	7.6
	1.00	247	7.5
	2.00	336	7.2
	5.00	500	6.8

[a] The solution was 0.1*M* TBAI in DMF. The platinum working electrode area was 0.11 cm². The value of $i_{pc}/v^{1/2}C$ for the reduction of azobenzene in these solutions at this electrode was 8.2, and was independent of scan rate. Experimental results of V. Puglisi.

Double potential step experiments.—To measure the rate at which the radical anion produced during the first reduction wave reacts and from these data elucidate the mechanism for the reaction, double potential step chronoamperometric experiments were undertaken. These methods, which have been used previously for reactions involving following first-order reactions (EC-mechanism) (8, 9), involve measuring the current as a function of time when the potential of the working electrode is changed.

Experimentally, the potential is first stepped to E_1, where the reaction $R + e \rightarrow R^{\cdot -}$ occurs at a mass transfer controlled rate. At a time T_F, the potential is stepped to E_2 where only the reaction $R^{\cdot -} \rightarrow R + e$ occurs. In chronoamperometric experiments, the current is measured just before T_F (I_F) and just before $2T_F$ (I_B). The ratio I_B/I_F has a value of 0.2928 in the absence of kinetic perturbations regardless of the length of T_F (8). If $R^{\cdot -}$ reacts to form nonoxdizable species, then the ratio I_B/I_F is perturbed, and will be a function of T_F. The order and rate of the perturbing reaction can be found from the variation of this ratio with T_F and concentration.

Chronocoulometric experiments are similar, except that Q_F and Q_B are measured at T_F and $2T_F$, respectively, with the unperturbed ratio Q_B/Q_F equal to 0.4142 (9).

Because the potential is stepped to values where the electrode reactions (either reduction of R or oxidation of $R^{\cdot -}$) occur at diffusion controlled rates, the measurement is unaffected by the rate of the electron transfer step. Moreover, when an adequate potentiostat and positive feedback compensation of uncompensated resistance are employed, the measurements are relatively unperturbed by double layer charging effects. These are decided advantages of these techniques over cyclic voltammetric investigations of the mechanism. Moreover, digital simulation of the different cases involving kinetic complications are somewhat easier for potential steps than for potential sweeps.

Five different reaction schemes were considered as possible in the hydrodimerization reaction scheme:

I. First order EC:

$$\text{At } E_1\text{: } R + e \rightarrow R^{\cdot -} \qquad R^{\cdot -} \xrightarrow{k_1} X$$
$$\text{At } E_2\text{: } R^{\cdot -} \rightarrow R + e$$

II. First order ECE

$$\text{At } E_1\text{: } R + e \rightarrow R^{\cdot -} \qquad R^{\cdot -} \xrightarrow{k_1} R^{\cdot -\prime};\ R^{\cdot -\prime} + e \rightarrow X$$
$$\text{At } E_2\text{: } R^{\cdot -} \rightarrow R + e$$

III. Second order EC

$$\text{At } E_1\text{: } R + 2e \rightarrow R^{2-} \qquad R^{2-} + R \xrightarrow{k_2} R_2^{2-}$$
$$\text{At } E_2\text{: } R^{2-} \rightarrow R + 2e$$

IV. Second order ECE

$$\text{At } E_1\text{: } R + e \rightarrow R^{\cdot -}$$
$$R^{\cdot -} + R \xrightarrow{k_2} R_2^{\cdot -};\ R_2^{\cdot -} + e \rightarrow R_2^{2-}$$
$$\text{At } E_2\text{: } R^{\cdot -} \rightarrow R + e$$
(For IVA: $R^{\cdot -} \rightarrow R + e$ and $R_2^{\cdot -} \rightarrow$ products + e)

V. Second order dimerization

$$\text{At } E_1\text{: } R + e \rightarrow R^{\cdot -} \qquad 2R^{\cdot -} \xrightarrow{k_2} R_2^{2-}$$
$$\text{At } E_2\text{: } R^{\cdot -} \rightarrow R + e$$

Schemes III, IV, and V represent possible alternate paths to the hydrodimer. It is assumed that R_2^{2-} is protonated rapidly, so that oxidation of R_2^{2-} at the

electrode at E_2 need not be considered. Similarly, the results would be the same in say V, if $R\cdot^-$ first protonated in a fast reaction and then the protonated species coupled to R_2H_2. Scheme II represents the case of, for example, protonation of $R\cdot^-$ followed by further reduction to lead to the two-electron product RH_2. Scheme I has been treated previously (8, 9) and was included here to compare with the other cases and also to serve as a check on our digital simulation procedure.

The digital simulation procedures for obtaining theoretical I-time (t) and Q-t curves generally followed methods described in detail before (10, 11). For simplicity, the diffusion coefficients of all species were taken as equal. The results are changed only slightly for reasonable differences in diffusion coefficients (*e.g.*, $D_{R^-} = 2D_{R_2^{2-}}$, etc.). The normalized currents or coulombs are determined as functions of the dimensionless parameter k_jTC^{j-1} (when $k_jT_FC^{j-1} = 1.0$), where j is the order of the reaction consuming $R\cdot^-$ ($j = 1$ for cases I and II and $j = 2$ for cases III, IV, and V) and C is the bulk concentration of R (Fig. 3). Variations in $k_jT_FC^{j-1}$ result in variations in the ratio I_B/I_F and Q_B/Q_F for each mechanism. As a result of several simulations with other values assigned to the parameter $k_jT_FC^{j-1}$, the ratios shown in Table II were obtained. From these tabulated data the working curves for the different mechanisms are drawn. To simplify evaluation of experimental results and to establish criteria that might distinguish between the proposed mechanisms, the working curves are plotted using the dimensionless ratio I_B/I_F, normalized by dividing by 0.2928, which we will call R_I, the normalized current ratio. This ratio will vary from 1.0 in the absence of kinetic complications to zero for large values of $k_jT_FC^{j-1}$. Similarly, the Q_B/Q_F ratio is normalized to yield an R_Q which varies between zero in the absence of kinetic perturbations to 1.0 in the limit of fast kinetics. (Where comparisons with previous theoretical treatments based on solution of the partial differential diffusion equations under appropriate boundary conditions are possible, excellent agreement is obtained.) The horizontal axis is given in units of $t_{1/2}$, the real time at which $R_I = 0.5$ (Fig. 4). This value of $t_{1/2}$ can be used to calculate the rate constant of the reaction, once the mechanism is established, by the expressions given in Table II. The different mechanisms can be distinguished by comparing the shape of experimental R_I or R_Q *vs.* $t_{1/2}$ curves with the theo-

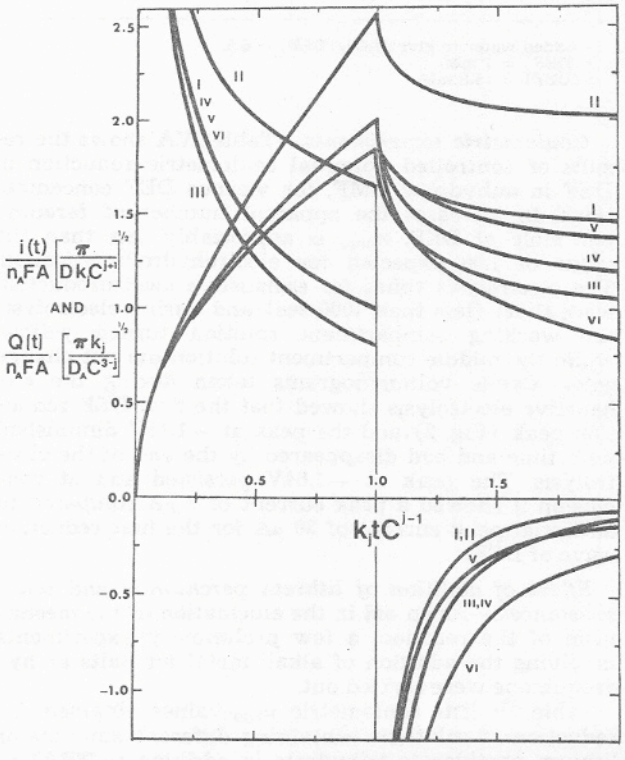

Fig. 3. Variation of current and coulombs with k_jtC^{j-1} for different mechanisms in text for double potential step chronoamperometry and chronocoulometry. VI represents system with no kinetic complications.

Table II. Values of normalized current (R_I) and coulomb (R_Q) ratios for different values of kT_FC for possible hydrodimerization reaction mechanisms[c]

k_1T_F	R_I (simulation)	R_I (lit)[a]	R_Q (simulation)	R_Q (lit)[b]
Mechanism I				
0.001	0.998		0.001	
0.050	0.917	0.918	0.043	0.029
0.100	0.842	0.844	0.083	0.082
0.200	0.709	0.711	0.157	0.154
0.300	0.598	0.601	0.223	0.219
0.400	0.505	0.508	0.283	0.278
0.500	0.427	0.429	0.337	0.332
0.700	0.305	0.308	0.430	0.423
0.900	0.219	0.222	0.506	0.499
1.00	0.186	0.188	0.539	0.532
1.30	0.114	0.116	0.621	0.612
1.70	0.060	0.062	0.701	0.693
Mechanism II				
0.001	0.997		0.002	
0.050	0.872	0.889	0.060	
0.100	0.765	0.770	0.114	
0.150	0.673	0.678	0.164	
0.200	0.595	0.603	0.211	
0.250	0.528	0.536	0.254	
0.300	0.470	0.478	0.294	
0.400	0.375	0.382	0.365	
0.500	0.302	0.309	0.427	
0.700	0.200	0.205	0.528	
1.00	0.112	0.115	0.638	
1.40	0.054	0.056	0.736	
k_2T_FC	R_I	R_Q		
Mechanism III				
0.001	0.999	0.001		
0.100	0.917	0.036		
0.250	0.812	0.085		
0.400	0.723	0.128		
0.700	0.582	0.202		
0.900	0.508	0.244		
1.00	0.475	0.263		
1.30	0.392	0.315		
1.80	0.289	0.385		
2.40	0.203	0.452		
3.50	0.110	0.543		
5.00	0.049	0.626		
Mechanism IV				
0.001	0.998	0.001		
0.100	0.893	0.045		
0.200	0.802	0.086		
0.300	0.723	0.123		
0.500	0.594	0.189		
0.700	0.495	0.246		
1.00	0.383	0.317		
1.30	0.302	0.377		
1.80	0.208	0.456		
2.90	0.099	0.577		
4.00	0.051	0.655		
Mechanism IVA				
1.25	0.249	0.526		
5.00	0.181	0.679		
10.00	0.141	0.761		
20.00	0.106	0.824		
30.00	0.090	0.852		
50.00	0.073	0.879		
100.00	0.056	0.907		
Mechanism V				
0.0005	0.989	0.001		
0.075	0.912	0.069		
0.200	0.798	0.162		
0.350	0.697	0.249		
0.500	0.619	0.316		
0.800	0.509	0.414		
1.00	0.456	0.463		
1.20	0.414	0.502		
2.00	0.306	0.608		
5.00	0.162	0.759		
12.5	0.079	0.058		
25.0	0.044	0.906		

[a] From ref. (8).
[b] From ref. (9); note, however, that a computational error appears to have been made computing the final results from the correct derived equation. The results in this column have been recomputed (J. Phelps, University of Texas at Austin, 1968).
[c] Rate constants can be calculated from the measured $t_{1/2}$-value by the following equations:

Mechanism	Rate constant
I	$k_1 = 0.406/t_{1/2}$
II	$k_1 = 0.273/t_{1/2}$
III	$k_2 = 0.922/t_{1/2}C$
IV	$k_2 = 0.690/t_{1/2}C$
V	$k_2 = 0.830/t_{1/2}C$

where $t_{1/2}$ is the value of T_F at which $R_I = 0.5$.

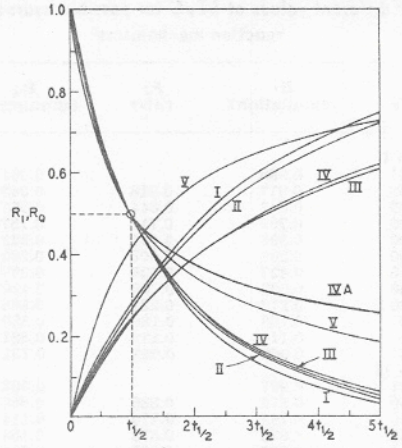

Fig. 4. Variation of normalized current and coulomb parameters as functions of $t_{1/2}$ for the different mechanisms in the text.

retical ones of Fig. 4. The following conclusions can be made about the possibility of distinguishing among mechanisms I through V: (*i*) the R_I and R_Q *vs.* T_F behavior for V is sufficiently different from the others to be distinguished; (*ii*) since I and II are independent of concentration, they may be distinguished from III and IV; (*iii*) it would be difficult to distinguish between III and IV only on the basis of potential step data; however, other information, such as the number of electrons involved in the electrode reaction determined at small times and low concentrations, or the establishment of the existence of intermediate radical ions by ESR can be used.

Double potential step chronoamperometric experiments were performed with several concentrations of DEF in DMF-TBAI solutions containing different amounts of water; typical results are given in Fig. 5 and Table III. The points shown in Fig. 5 fall along a theoretical curve characteristic of mechanism V, values of the rate constant for dimerization of the radical anions, k_2, are given in Table III. Note that the data do not fit the R_I *vs.* t behavior characteristic of the other mechanisms, particularly for times greater than several half-lives. For example, for mechanism IV, at a $T_F = 5\ t_{1/2}$, R_I is less than 0.07, whereas experimentally, R_I values of about 0.19 are found. Within the framework of mechanisms considered, the type involving formation of radical ions and then coupling of these gives the best agreement with theory. Addition of water increases the rate of this coupling reaction, but does not appear to alter the over-all mechanism.

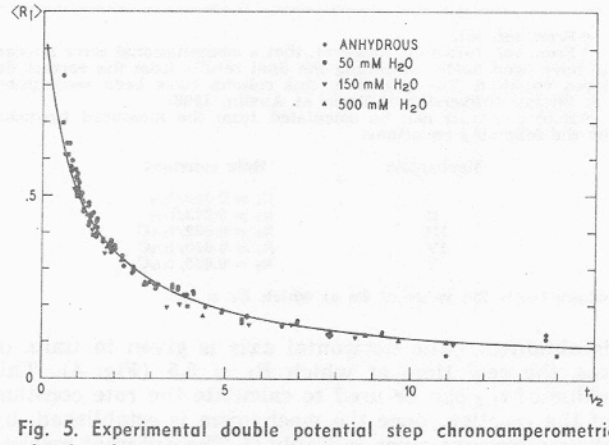

Fig. 5. Experimental double potential step chronoamperometric results for the reduction of a 10 mM solution of DEF in 0.10M TBAI in DMF solutions with different amounts of water added. The points are experimental and the line shows the simulation results of mechanism V.

Table III. Results of double potential step chronoamperometric investigation of diethyl fumarate hydrodimerization[a]

Water concentration	$-E_{p/2}$ (V *vs.* Ag reference)	k_2 [b] (l/mole-sec)	$it^{1/2}$ [c] (μA-sec$^{1/2}$)
Anhydrous	0.76	37	23
Anhydrous[d]	—	30.5	—
Anhydrous[d,e]	—	15.5	—
50 mM	0.75	46	24
150 mM	0.76	57	23
500 mM	0.74	145	23

[a] The solution contained 0.2M tetra-n-butylammonium iodide (TBAI) in dimethylformamide (DMF) and 10.0 mM diethyl fumarate (DEF). The potential program was −0.2V, −1.0V (E_1), −0.2V (E_2) *vs.* silver wire reference electrode. The temperature was 25° ± 1°C.
[b] For dimerization of $R\cdot$.
[c] For forward step.
[d] 9.75 mM DEF, 0.10*M* TBAI.
[e] Temperature was 0°C.

Table IV. Controlled potential coulometry results for the reduction of diethyl fumarate

A. Solution containing 0.43*M* TBAI in DMF

Diethyl fumarate concentration (mM)	n_{app}
4.67	0.76
6.00	0.76
10.0	0.61
17.7	0.64
24.0	0.64

B. Solution containing about 10 m*M* DEF and 0.44*M* TBAI in DMF with different amounts of $LiClO_4 \cdot 3H_2O$

$[LiClO_4 \cdot 3H_2O]/[DEF]$	n_{app}
0.0	0.61
0.50	0.80
0.50[a]	0.82
0.89	0.91
1.93	0.98
2.12	0.94
3.24	0.96
3.9	0.99

C. Solution containing 0.44*M* TBAI in DMF with other additives

$[NaI]/[DEF] = 2.0$[b]	0.62
$[NaI + 3H_2O]/[DEF] = 2.0$[b]	0.63
[Hydroquinone]/[DEF] = 2.0[c]	1.32

[a] Added water to give $[H_2O]/[DEF] = 6.5$.
[b] [DEF] = 1 mM.
[c] [DEF] = 16.8 mM.

Coulometric experiments.—Table IVA shows the results of controlled potential coulometric reduction of DEF in anhydrous DMF, for various DEF concentrations. In all cases the apparent number of faradays per mole of DEF, n_{app}, is appreciably less than the value of 1.00 expected for electrohydrodimerization. The electrolysis times for exhaustive electroreduction were short (less than 1000 sec) and during electrolysis the working compartment solution turned yellow, while the middle compartment solution did not change color. Cyclic voltammograms taken during the exhaustive electrolysis showed that the first DEF reduction peak (Fig. 2) and the peak at −1.45V diminished with time and had disappeared by the end of the electrolysis. The peak at −1.64V persisted and at conclusion it showed a peak current of 7 μA compared to an initial peak current of 30 μA for the first reduction wave of DEF.

Effect of addition of lithium perchlorate and other substances.—As an aid in the elucidation of the mechanism of the reaction, a few preliminary experiments involving the addition of alkali metal ion salts or hydroquinone were carried out.

Table IV lists coulometric n_{app}-values obtained for reduction of solutions containing different amounts of lithium perchlorate trihydrate in addition to TBAI in DMF, for DEF of about 1 mM. These data are shown graphically in Fig. 6. As the ratio of $LiClO_4 \cdot 3H_2O$ to DEF approaches about 2.0, the n_{app}-value increases to the value of 1.0 expected for the hydrodimerization reaction as the sole reaction. For ratios of about 2.0 and

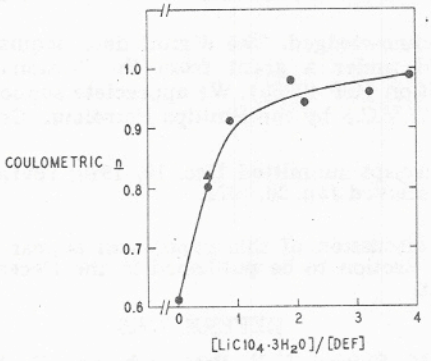

Fig. 6. Coulometric n_{app}-values for the reduction of DEF in solutions containing various ratios of lithium perchlorate trihydrate to DEF. The solutions contained 10 mM DEF. The point marked △ contained additional water to give $[H_2O]/[DEF] = 6.5$.

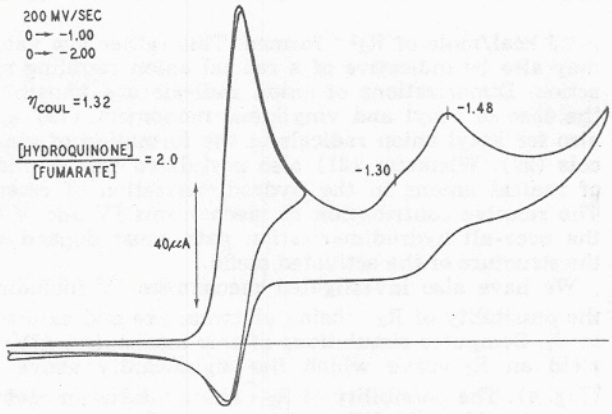

Fig. 8. Cyclic voltammograms for DEF solutions containing hydroquinone.

greater the total electrolysis times were typically 4000 sec as compared to shorter electrolysis times in anhydrous-DMF, or for low $LiClO_4 \cdot 3H_2O$/DEF ratios. The solution after reduction was water white for higher amounts of $LiClO_4 \cdot 3H_2O$, as compared to the yellow solutions characteristic of solutions containing no or low amounts of this salt. In one experiment at a $LiClO_4 \cdot 3H_2O$/DEF ratio of 0.50, water was added to give a water to DEF ratio of 6.5. This corresponds to the amount of water present in solutions with $LiClO_4 \cdot 3H_2O$/DEF ratios greater than 2.0. If the role of the lithium ion was only to catalyze a reaction with water, the coulometric n_{app} should approach 1.0. Experimentally, the n_{app}-value found was not significantly different from those found in solutions containing no additional water.

The cyclic voltammetric behavior of DEF is also altered by the presence of $LiClO_4 \cdot 3H_2O$ (Fig. 7). For $LiClO_4 \cdot 3H_2O$/DEF ratios of 1.9 or higher, no back current is observed for the oxidation of the reduction product of the first wave, for scan reversal at potentials of −1.0 to −1.7V *vs.* Ag-RE. Filming of the electrode occurs when the reduction scan is carried out to potentials beyond about −1.5V; evidence for this filming is the greatly decreased reduction currents on second and subsequent cathodic scans following reversal at these potentials. Normal (nonfilming) behavior for subsequent cathodic scans is observed for scans reversed at potentials up to −1.0V. At lower $LiClO_4 \cdot 3H_2O$/DEF ratios, some reversal current is observed after the first wave.

Controlled potential coulometry results for the addition of sodium iodide, and sodium iodide and water (Table IVC) show that lithium ion has a specific effect. The n_{app}-values with both NaI and H_2O are very close

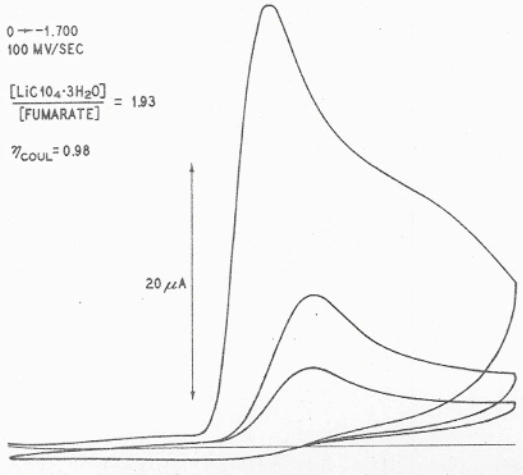

Fig. 7. Cyclic voltammograms for DEF solutions containing lithium perchlorate trihydrate.

to those in anhydrous DMF. Cyclic voltammograms with NaI, however, are very similar to those with $LiClO_4 \cdot 3H_2O$ (Fig. 7); they show the distortion following the fumarate reduction, the absence of back current on reversal following the first reduction wave, and the apparent filming of the electrode when cycled beyond −1.5V.

When hydroquinone is added as a proton donor in a coulometric experiment, an n_{app}-value larger than one is obtained. Cyclic voltammetry in the presence of hydroquinone (Fig. 8) as compared to that in its absence (Fig. 2) shows that the peak at −1.64V is absent, the peak at −1.45V persists and may show some reversibility, and a small peak at −1.30V is clearly detectable. The peak anodic current following reversal at −1.0V is smaller for solutions containing hydroquinone at the same DEF concentrations, while the cathodic peak current for the first reduction wave is about 12% larger.

Discussion

In agreement with Baizer and co-workers (3), we find the first step of the reduction to be a one-electron transfer to form the anion radical of DEF ($R \cdot^-$). Evidence for this includes the cyclic voltammetric $i_p/v^{1/2}$ C-value, which is very near that for the reduction of azobenzene in DMF, a known one-electron reduction (12). Moreover, electron spin resonance spectra of $R \cdot^-$ have been observed (13, 14). The double potential step experiments suggest that dimerization of these radical ions is the major path to the hydrodimer for DEF. Rejection of this dimerization step in the previous study (3) was based primarily on the rather large decrease of $i_p/v^{1/2}$ values with increasing v, which the authors felt favored an ECE-type reaction. However, the particular type of ECE-reaction which might occur (a second order ECE, mechanism IV) is different from the more usual first order ECE reaction (mechanism II) in that $n_{app} = 1$ at the limit of both very large and very small values of k_2 for mechanism IV, (whereas n_{app} varies between 1 and 2 as k_1 increases, for mechanism II). Several theoretical papers on linear potential sweep and cyclic voltammetry have recently appeared (15-18) which pertain to these mechanisms. In particular they show that the dimerization mechanism (scheme V) shows a decrease of $i_p/v^{1/2}$ of up to 18% with increasing v (15, 17), while the second-order ECE mechanism (scheme IV) shows a small increase in this function with increasing scan rate. An excellent comparison of these two mechanisms can be seen in Fig. 6 of the paper of Saveant *et al.* (17). Hence, the cyclic voltammetric data in this paper and in ref. (3) are in better agreement with the dimerization mechanism, although more detailed cyclic voltammetric experiments are required to test the extent of agreement quantitatively. The free energy of activation of the coupling process was determined from the measured rate constants at 25° and 0°C to be about

−4.5 kcal/mole of R_2^{2-} formed. This rather low value may also be indicative of a radical anion coupling reaction. Dimerizations of anion radicals are known in the case of vinyl and vinylidene monomers (19) and also for ketyl anion radicals in the formation of pinacols (20). Wiemann (21) also postulated the coupling of radical anions in the hydrodimerization of esters. The relative contribution of mechanisms IV and V to the over-all hydrodimerization path must depend on the structure of the activated olefin.

We have also investigated mechanism IV including the possibility of $R_2\overline{\cdot}$ being electroactive and oxidized at E_2. Computer simulations of this mechanism (IVA) yield an R_I curve which lies significantly above V (Fig. 4). The possibility of $R_2\overline{\cdot}$ having diffusion coefficients significantly different from the other species was also simulated. For example, curve IV is even higher above V when D_{R_2-} is smaller than D_R, so that mechanism IVA does not agree with our experimental data.

In agreement with Baizer and co-workers (3), we find that water increases the rate of disappearance of the anion radicals. This occurs without apparently causing a change in mechanism. Although this could be ascribed to fast protonation of $R\overline{\cdot}$ to RH· followed by dimerization, this seems unlikely, since RH· should also be reduced at the electrode (or by $R\overline{\cdot}$) in an ECE reaction (mechanism II) and no evidence for the involvement of this reaction is observed, even in coulometric experiments. Since the amounts of water which affect the reaction are too small to change the bulk dielectric constant appreciably, the rate increase may be due to specific solvation of the anion radicals by water. Hydroquinone, a better proton donor than water, does show a contribution of the first-order ECE mechanism both in voltammetric and coulometric experiments.

Polymerization, probably by reaction of R with R_2^{2-}, can account for the low n_{app}-values in coulometry. This reaction may not be important in the potential step experiments, since the solution in the vicinity of the electrode is relatively depleted in R. Lithium ion decreases the extent of this polymerization, perhaps by increasing the rate of protonation of R_2^{2-}.

Acknowledgment

The support of the Robert A. Welch Foundation and the National Science Foundation (GP 6688X) is gratefully acknowledged. The digital data acquisition was acquired under a grant from the National Science Foundation (GP 10360). We appreciate support for one of us (W.V.C.) by the Phillips Petroleum Company.

Manuscript submitted Dec. 10, 1970; revised manuscript received Jan. 20, 1971.

Any discussion of this paper will appear in a Discussion Section to be published in the December 1971 JOURNAL.

REFERENCES

1. M. M. Baizer, J. P. Petrovich, and D. A. Tyssee, *This Journal*, **117**, 173 (1970).
2. J. P. Petrovich, M. M. Baizer, and M. R. Ort, *ibid.*, **116**, 749 (1969).
3. J. P. Petrovich, M. M. Baizer, and M. R. Ort, *ibid.*, **116**, 743 (1969).
4. F. Beck, *Chem.-Ing. Tech.*, **37**, 607 (1965).
5. L. R. Faulkner and A. J. Bard, *J. Am. Chem. Soc.*, **90**, 6284 (1968).
6. G. Lauer, R. Abel, and F. C. Anson, *Anal. Chem.*, **39**, 765 (1967).
7. G. Lauer and R. A. Osteryoung, *ibid.*, **38**, 1137 (1966).
8. W. M. Schwarz and I. Shain, *J. Phys. Chem.*, **69**, 30 (1965); **70**, 845 (1966).
9. J. H. Christie, *J. Electroanal. Chem.*, **13**, 79 (1967).
10. S. Feldberg, "Electroanalytical Chemistry," Vol. 3, A. J. Bard, Editor, Marcel Dekker, Inc., New York (1969).
11. S. A. Cruser and A. J. Bard, *J. Am. Chem. Soc.*, **91**, 267 (1969).
12. J. L. Sadler and A. J. Bard, *ibid.*, **90**, 1979 (1968).
13. S. F. Nelson, *Tetrahedron Letters*, **39**, 3795 (1967).
14. I. Goldberg and A. J. Bard, Unpublished investigation, The University of Texas, 1969.
15. M. L. Olmstead, R. G. Hamilton, and R. S. Nicholson, *Anal. Chem.*, **41**, 260 (1969).
16. R. S. Nicholson, *ibid.*, **37**, 667 (1965).
17. C. P. Andrieux, L. Dadjo, and J. M. Saveant, *J. Electroanal. Chem.*, **26**, 147 (1970).
18. J. M. Saveant and E. Vianello, *Electrochim. Acta*, **12**, 1545 (1967).
19. M. Szwarc, "Carbanions, Living Polymers and Electron Transfer Processes," p. 367 *et. seq.*, Interscience, New York (1968).
20. C. K. Mann and K. K. Barnes, "Electrochemical Reactions in Nonaqueous Solvents," Chap. 6, Marcel Dekker, Inc., New York (1970).
21. J. Wiemann, *Bull. Soc. Chim. France*, **1964**, 2545.